snpAD: an ancient DNA genotyper

Supplementary Tables and Figures

June 19, 2018

Contents

List of Figures

List of Tables

1 Figures

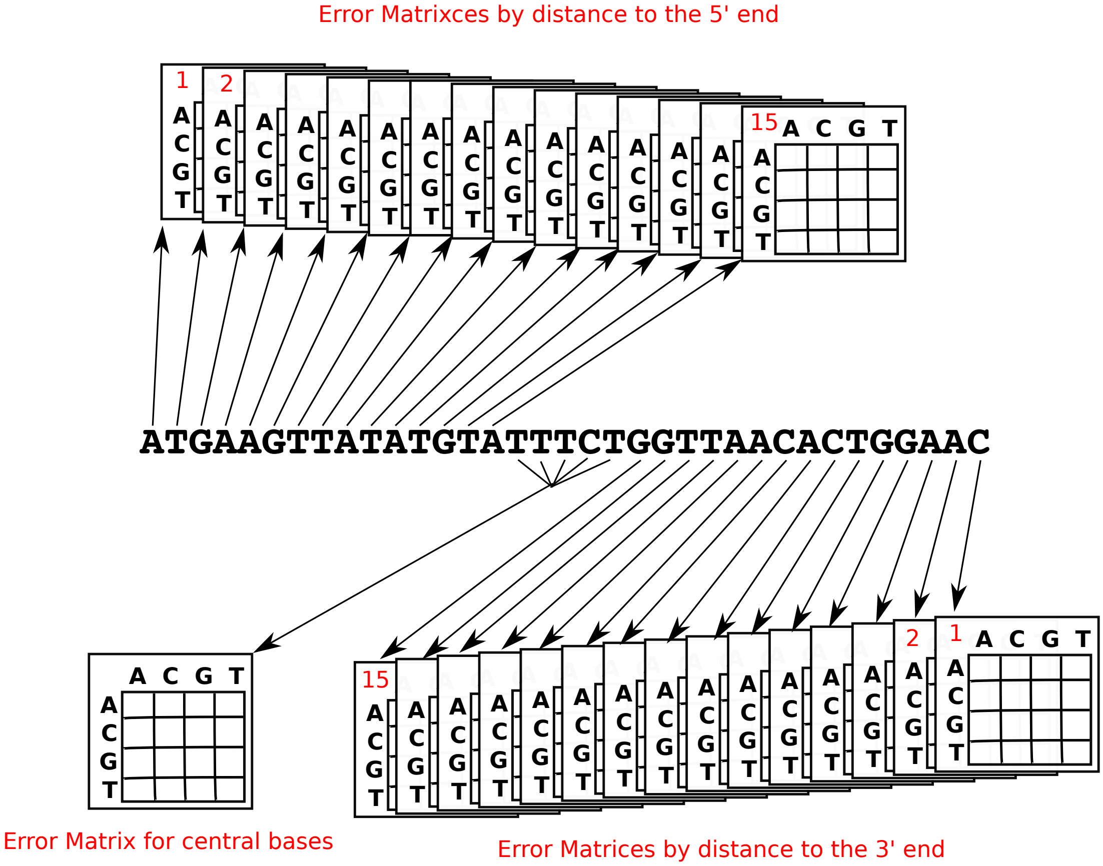
Error Matrixces by distance to the 5' end
1
2
15
A C G T
A
C
G
T
ATGAAGTTATATGTATTTCTGGTTAACACTGGAAC
Error Matrix for central bases
Error Matrices by distance to the 3' end

Figure 1: Schematic description of default error model. The first 15 and last 15 bases of each sequence are represented by separate base substitution matrices. Bases in the interior are assigned to a 31st matrix. This schema is expected to capture differences in substitution probabilities caused by ancient DNA damage (see e.g. Figs.12 and 13).

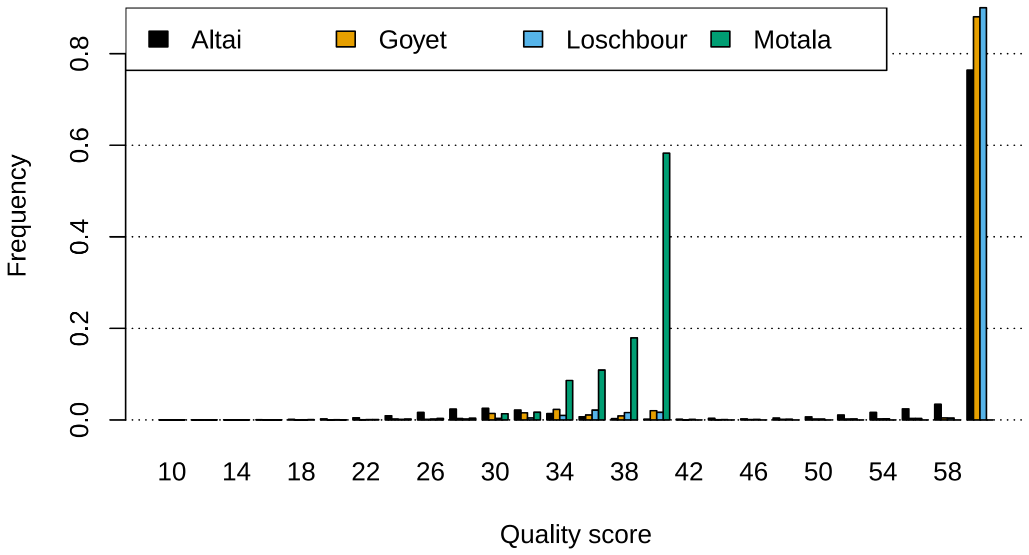

Figure 2: Histogram of quality scores in ancient samples: The majority of bases are of high-quality ($Q \geq 30$). See Table 1 for a description of the samples. Note that the maximum quality score is 40 in the Motala12 data and 60 for all other samples.

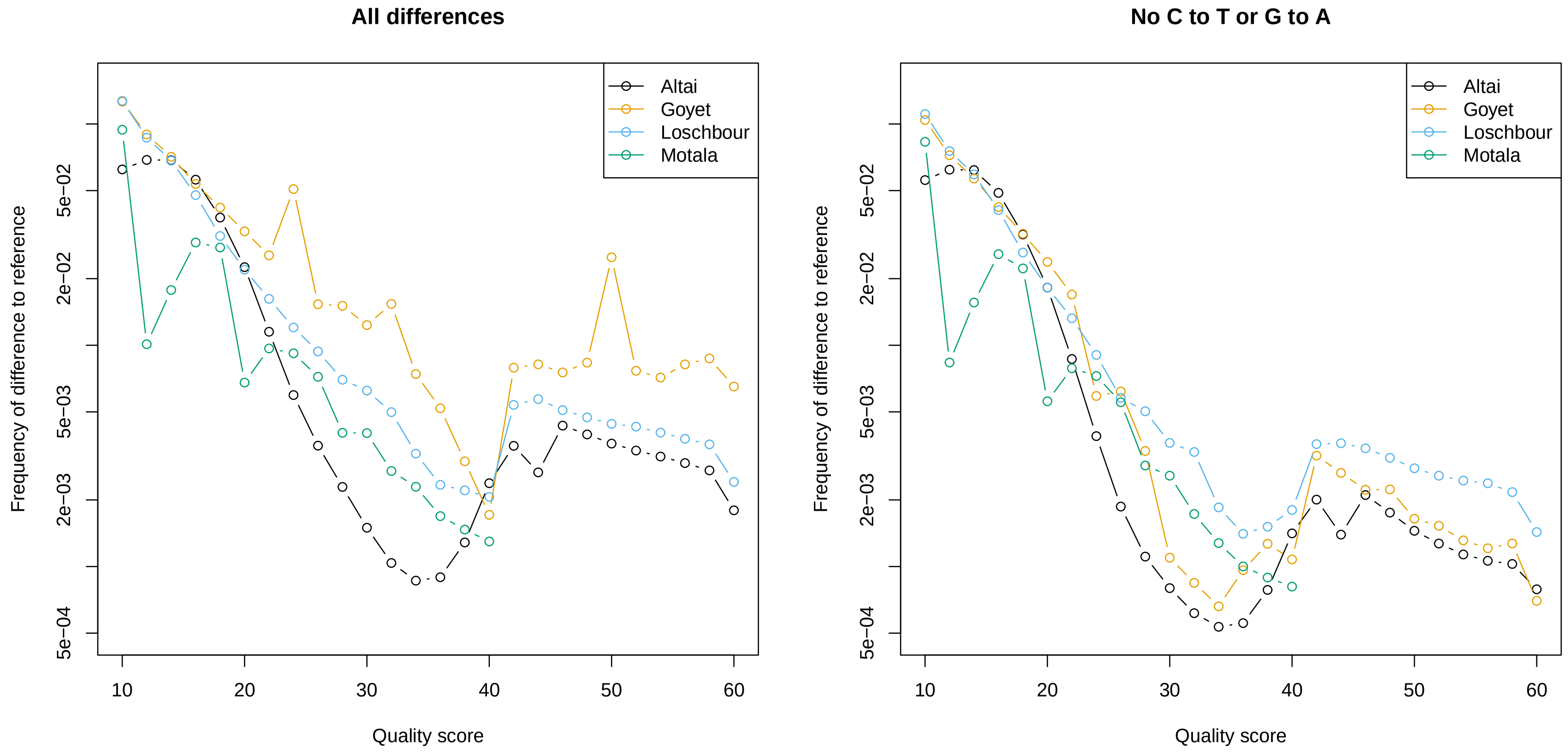

Figure 3: Effect of quality score filtering on pairwise sequence divergence for ancient samples. Shown are the average number of mismatching bases to a reference genome for all substitutions (left) and for any substititution, except for reference C to sample T or reference G to sample A (right). Note that the y-scale is on a log scale, and that increasing quality scores are expected to produce a linear decrease on that scale. The Altai and Goyet Neandertal samples were compared to the Altai genotype calls excluding heterozygous positions. Loschbour and Motala were compared to the human genome hg19. Analysis was restricted to chromosome 1 for low-coverage and chromosome 21 for high-coverage samples. See Supplementary Figure S7 in Prüfer *et al.* (2017) for a similar analysis of Vindija 33.19.

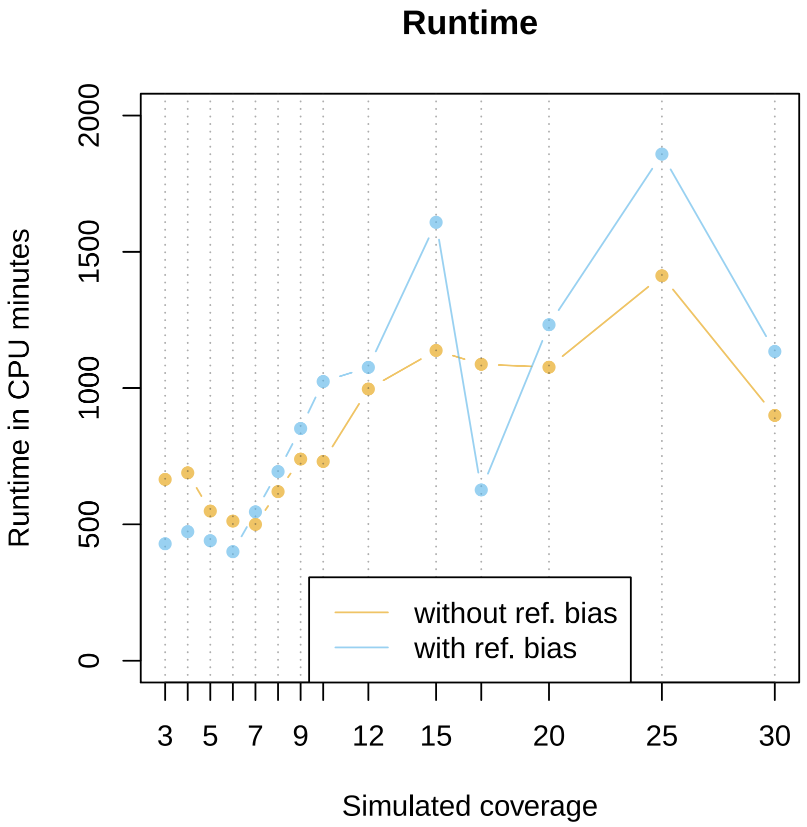

Figure 4: Runtime in CPU minutes for estimates with and without reference bias on simulated datasets. Wall clock time ranged from 23 to 83 minutes parellelizing over 30 cores of a multi-core Intel Xeon server.

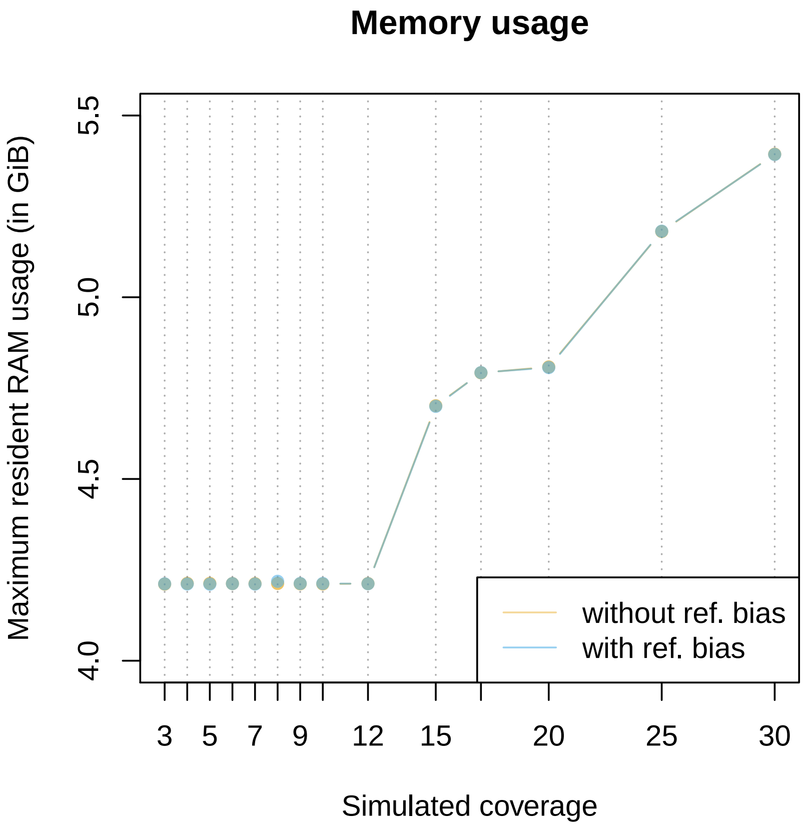

Figure 5: Maximum RAM usage in GiB during estimation of parameters with and without reference bias on simulated datasets. Note that the estimates overlap almost perfectly between the runs with and without reference bias so that points appear in light gray. Y-axis starts at 4GiB.

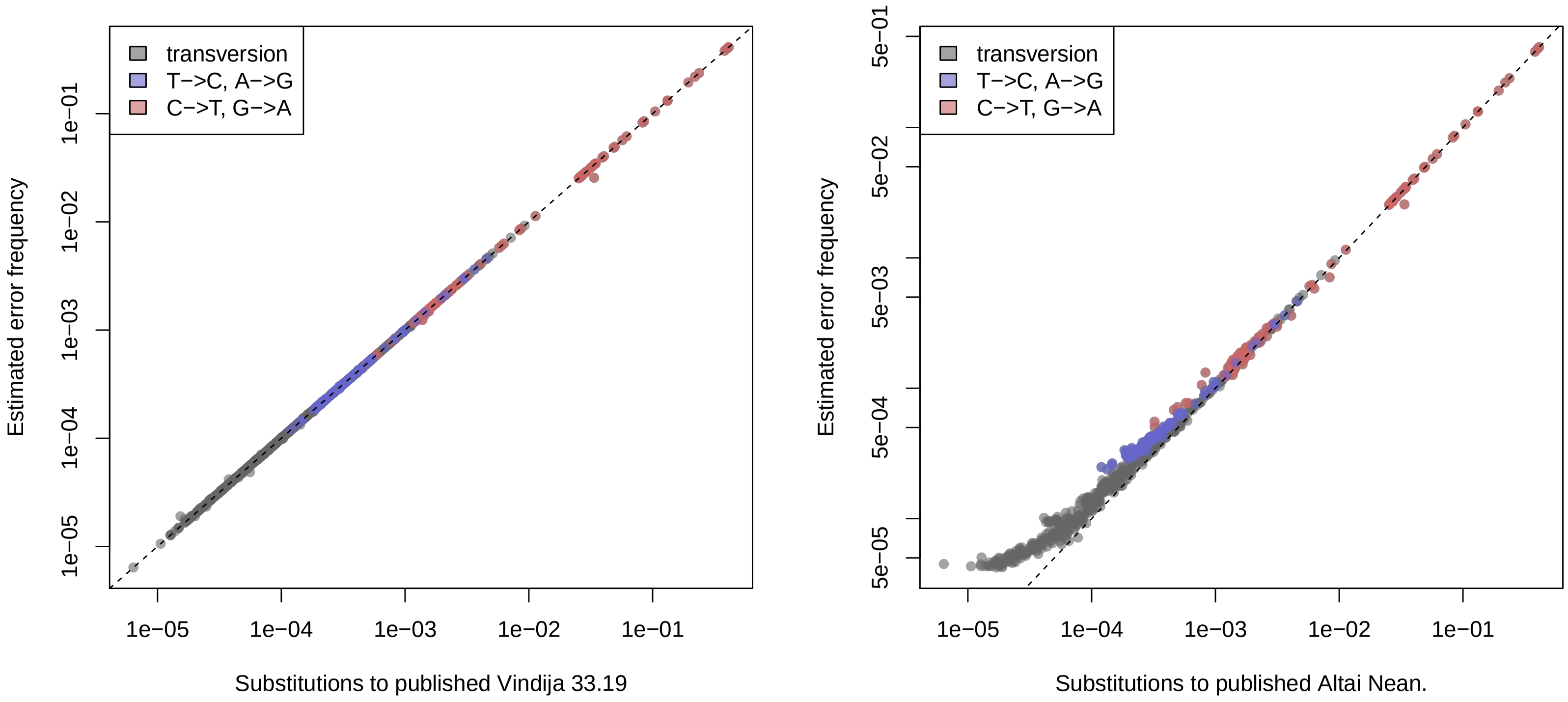

Figure 6: Error estimates for Vindija 33.19 data on chromosome 21. Left: Error estimates compared to substitutions of the Vindija 33.19 sequences to the previously published Vindija 33.19 genotypes. Right: Error estimates compared to substitutions of the data to the Altai Neandertal genotypes.

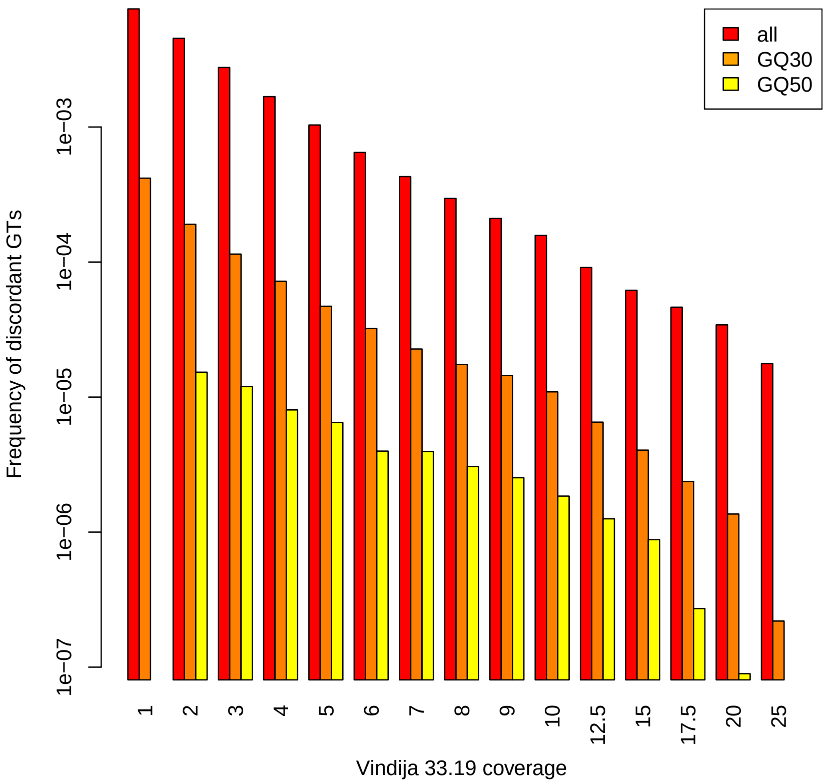

Figure 7: Discordant genotype calls in Vindija 33.19 subsamples compared to the full 30x coverage calls. Frequency of discordant genotypes is on a log-scale. Colors indicate whether all genotypes were considered, or only those with a genotype quality >30 or >50.

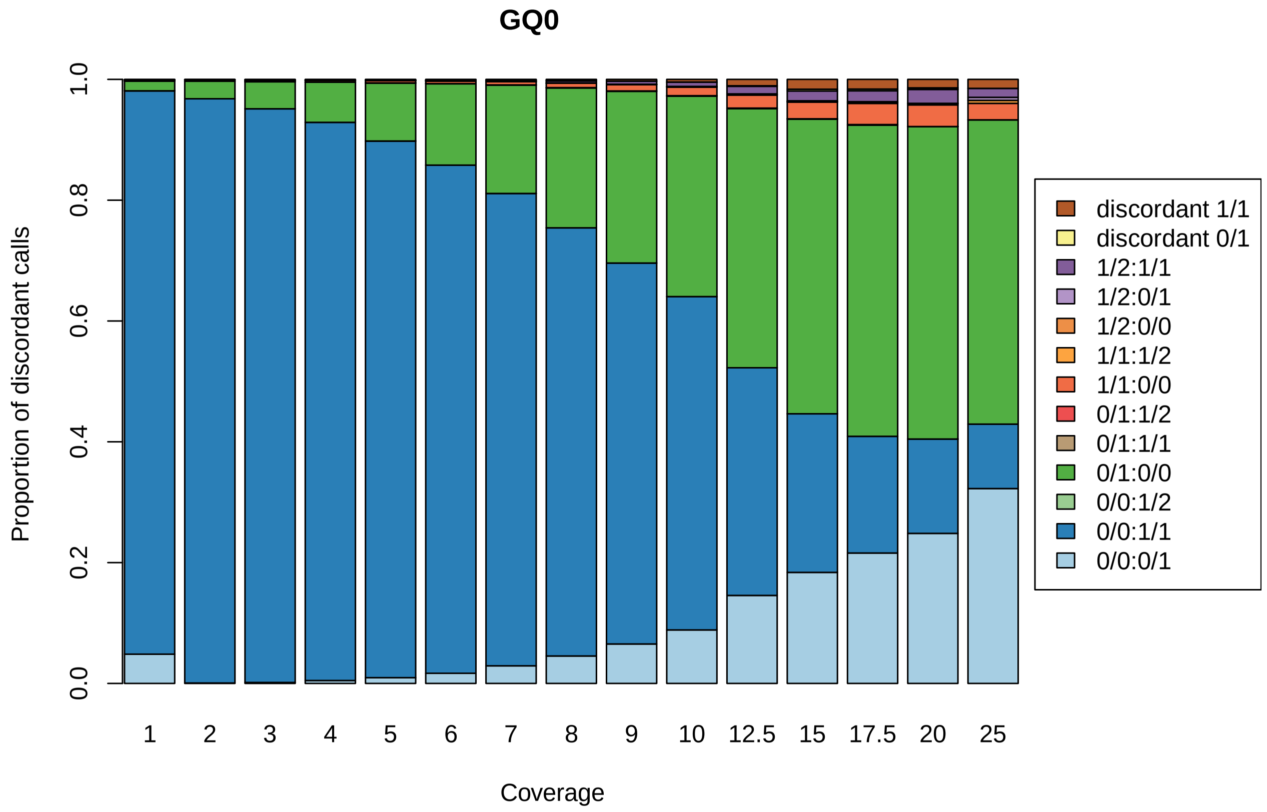

Figure 8: Classification of discordant genotype calls in Vindija 33.19 subsamples. No genotype quality cutoff was applied. For counts see Table 13. Legend shows genotypes in order 30x:subsample.

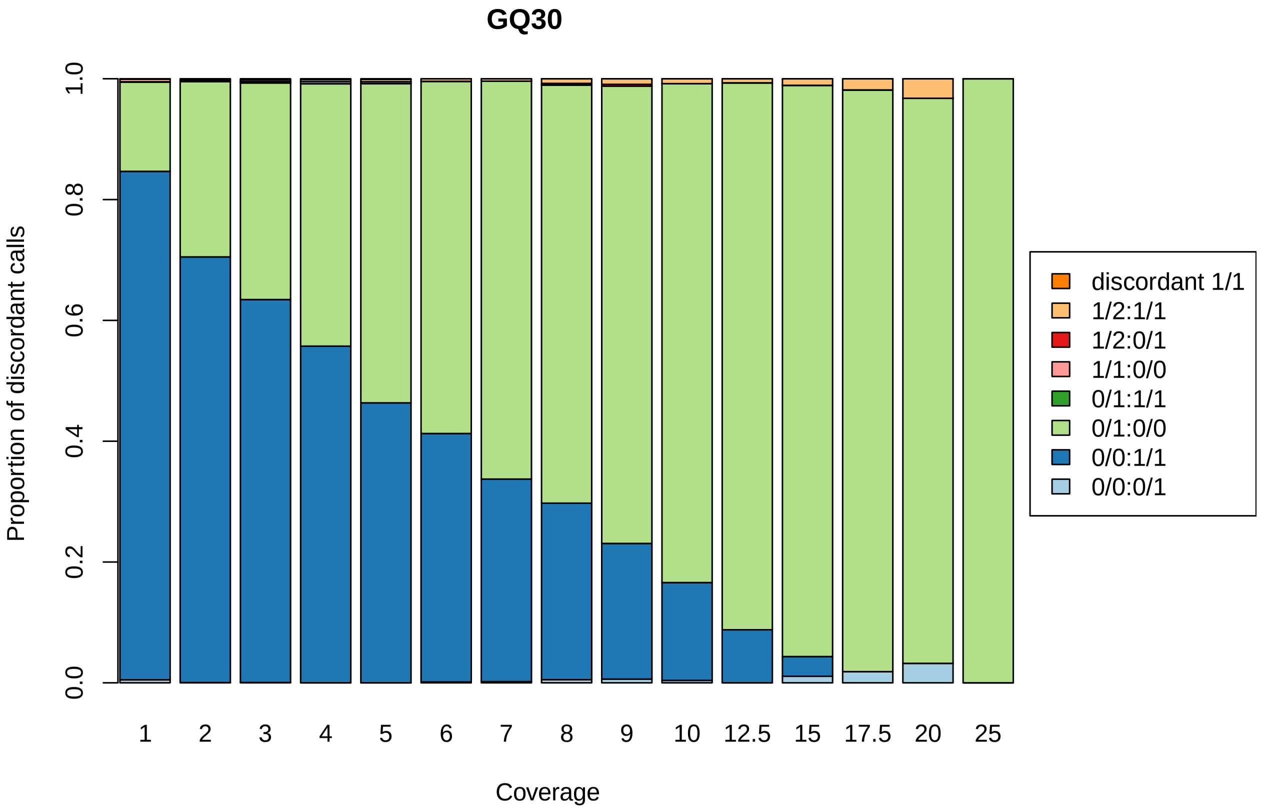

Figure 9: Classification of discordant genotype calls in Vindija 33.19 subsamples. A genotype quality cutoff of ≥30 was applied. For counts see Table 13. Legend shows genotypes in order 30x:subsample.

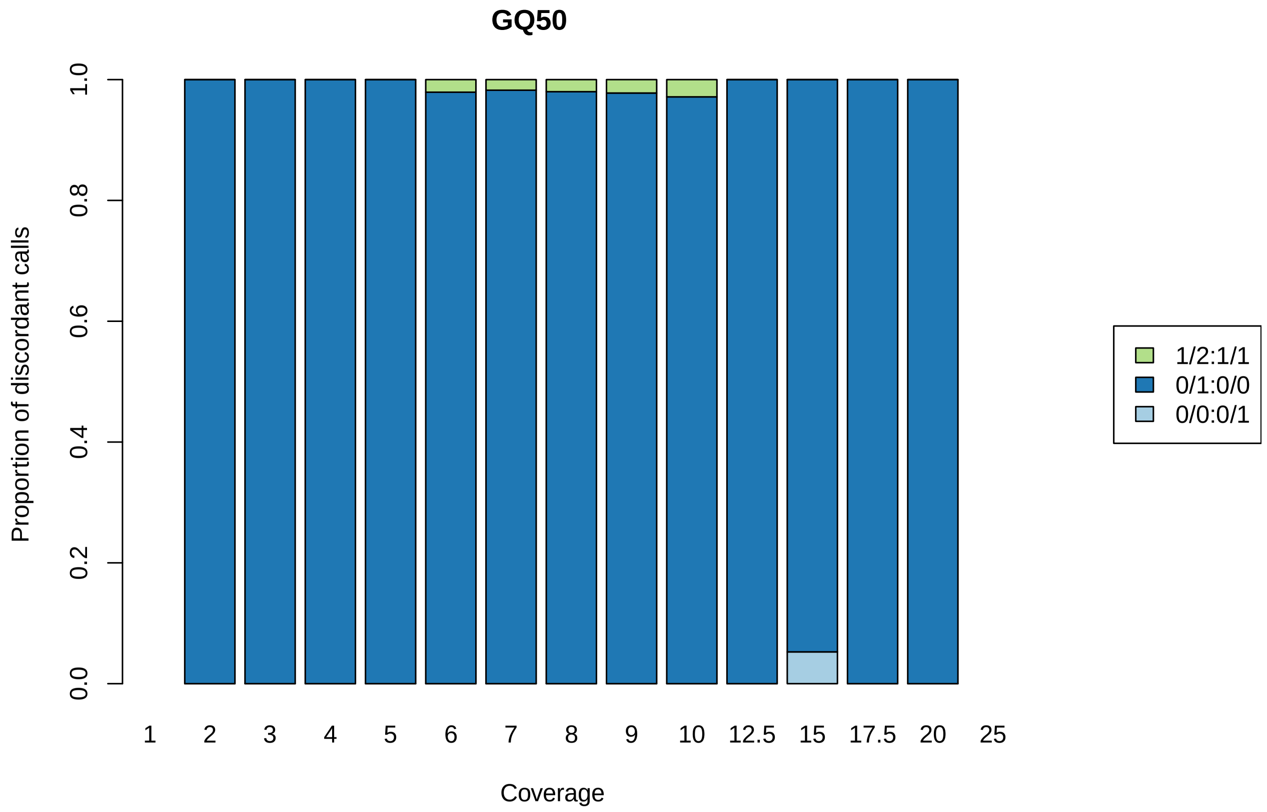

Figure 10: Classification of discordant genotype calls in Vindija 33.19 subsamples. A genotype quality cutoff of $\geq$50 was applied. No discordant calls were observed for coverage 1 and 25. For counts see Table 13. Legend shows genotypes in order 30x:subsample.

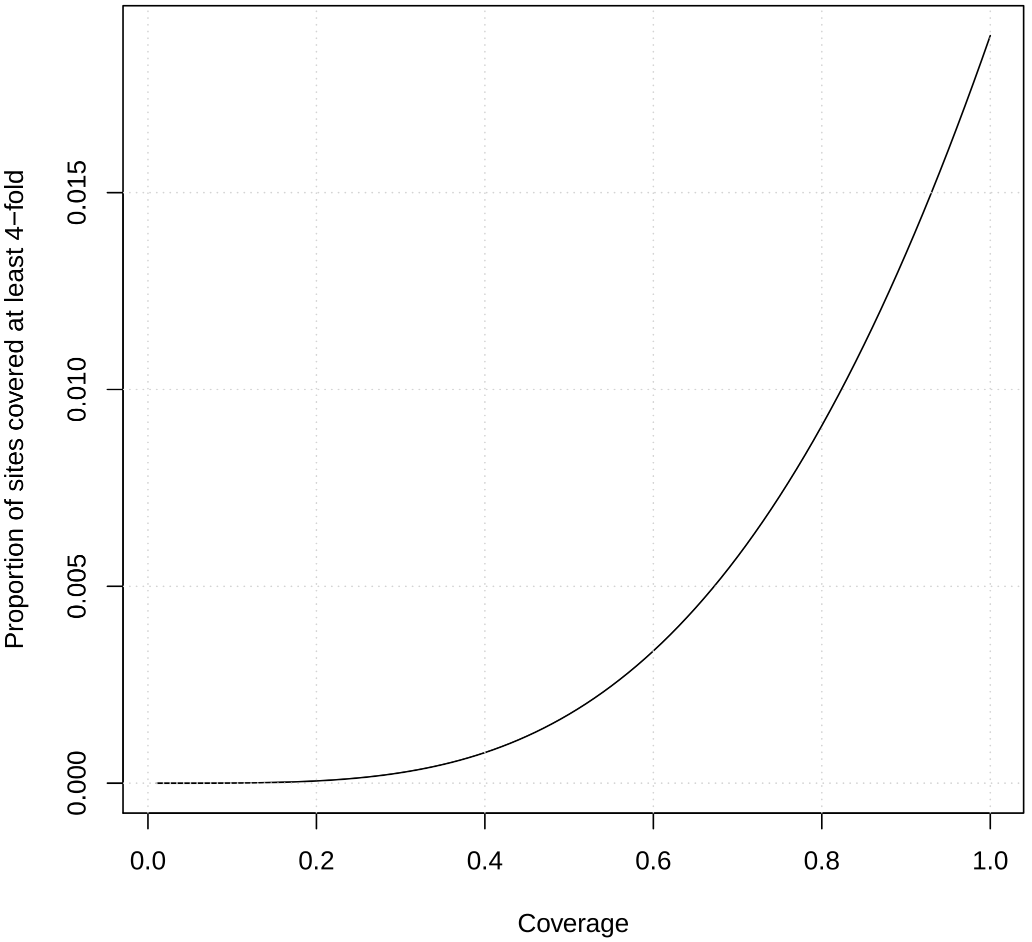

Figure 11: Expected proportion of sites with at least 4-fold coverage in low-coverage genomes according to the Lander-Waterman statistics.

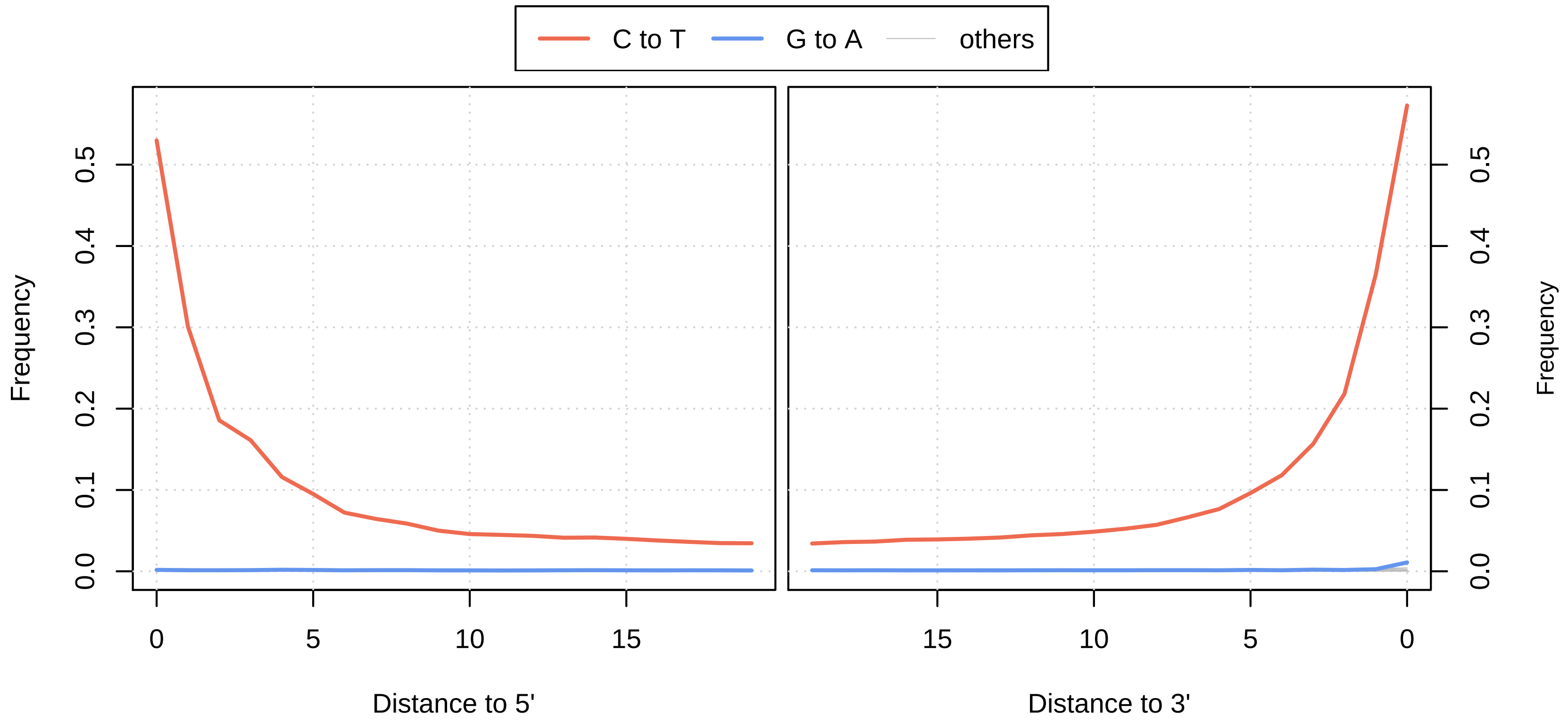

Figure 12: Damage patterns in the Vindija 87 Neandertal data prepared with a single stranded library protocol.

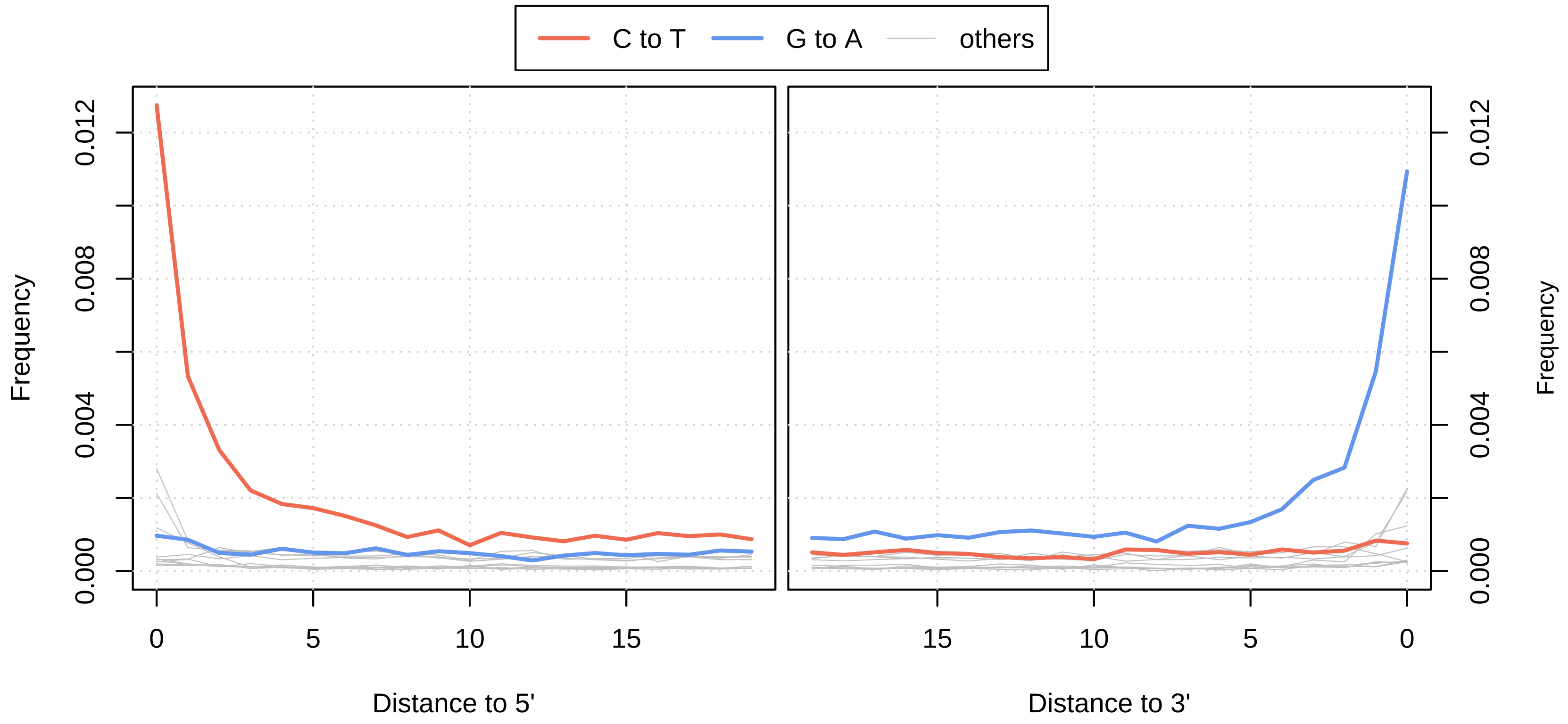

Figure 13: Damage patterns in the data of the European hunter-gatherer Motala12 prepared with a double stranded library protocol.

2 Tables

Group	Name	Coverage	Reference
Neandertal	Altai (from Denisova cave)	52x	Prüfer *et al.* (2014)
Neandertal	Vindija 33.19	30x	Prüfer *et al.* (2017)
Modern human	Loschbour	22x	Lazaridis *et al.* (2014)
Neandertal	Les Cottés Z4-1514	2.7x	Hajdinjak *et al.* (2018)
Modern human	Motala 12	2.4x	Lazaridis *et al.* (2014)
Neandertal	Goyet Q56-1	2.2x	Hajdinjak *et al.* (2018)
Neandertal	Mezmaiskaya 2	1.7x	Hajdinjak *et al.* (2018)
Neandertal	Vindija 87	1.3x	Hajdinjak *et al.* (2018)
Neandertal	Spy 94a	1.0x	Hajdinjak *et al.* (2018)

Table 1: Datasets used in this study.

Cov.	AC	AG	AT	CG	CT	GT
3	0.0994	0.193	0.0979	0.0958	0.197	0.0977
4	0.0983	0.2045	0.1008	0.0977	0.2074	0.1056
5	0.0987	0.2035	0.105	0.1006	0.2051	0.092
6	0.1001	0.1973	0.1002	0.103	0.2035	0.0975
7	0.0998	0.2004	0.1001	0.1024	0.2083	0.1037
8	0.103	0.1964	0.1007	0.1014	0.1985	0.0961
9	0.0966	0.2057	0.0916	0.0972	0.1986	0.095
10	0.1039	0.1952	0.096	0.1	0.2053	0.1003
12	0.1051	0.2022	0.1	0.0949	0.2033	0.0989
15	0.0994	0.1985	0.1009	0.099	0.2003	0.1027
17	0.1014	0.2019	0.0992	0.0993	0.2026	0.0964
20	0.099	0.1939	0.1018	0.0998	0.2012	0.1031
25	0.1045	0.2009	0.0971	0.0964	0.2007	0.0986
30	0.0976	0.2051	0.1019	0.0974	0.2011	0.0976

Table 2: Simulated genotype frequencies (per 1000bp). Deviation from specified parameters are due to the use of a pseudo random number generator during simulation.

Cov.	AC	AG	AT	CG	CT	GT
3	0.141943	0.487617	0.132684	0.217547	0.518872	0.145262
4	0.0978802	0.217037	0.106058	0.103366	0.207338	0.107778
5	0.0977911	0.19909	0.102525	0.0982538	0.213814	0.0922814
6	0.0982396	0.2003	0.100129	0.100975	0.2039	0.0957835
7	0.0994662	0.205249	0.099413	0.101335	0.211202	0.102465
8	0.102891	0.202079	0.100336	0.101366	0.195546	0.0962143
9	0.0961095	0.201015	0.0916744	0.0967756	0.198276	0.0956978
10	0.102898	0.195699	0.0955418	0.10141	0.209569	0.100444
12	0.105482	0.200895	0.100301	0.0951686	0.204228	0.0986684
15	0.0998465	0.199688	0.100235	0.0986095	0.199992	0.10304
17	0.101299	0.202168	0.0993153	0.0990021	0.201701	0.0962989
20	0.0985454	0.194164	0.101311	0.099694	0.200358	0.103154
25	0.104501	0.200799	0.0970826	0.0963994	0.200622	0.0985396
30	0.0976482	0.20494	0.101913	0.0973725	0.201186	0.0976336

Table 3: Estimated genotype frequencies (per 1000bp) from simulations (see Table 2).

Genotype	Simulated freq.	Estimated freq.	Exp-Obs/Exp
AC	0.10027	0.132199	-0.318
AG	0.19781	0.242159	-0.224
AT	0.10025	0.020440	0.7961
CG	0.10238	0.230882	-1.255
CT	0.19831	0.235709	-0.189
GT	0.10012	0.131489	-0.313

Table 4: Estimated genotype frequencies (per 1000bp) from a simulation with 100 million sites at exactly 3-fold coverage.

Genotype	Simulated freq.	Estimated freq. with true error rates	Exp-Obs/Exp
AC	9.94e-05	9.67491e-05	0.026669014084507
AG	0.000193	0.000178968	0.0727046632124353
AT	9.79e-05	9.88342e-05	-0.00954239019407561
CG	9.58e-05	9.81046e-05	-0.0240563674321503
CT	0.000197	0.000211775	-0.0750000000000001
GT	9.77e-05	0.000102151	-0.0455578300921188

Table 5: Genotype frequency estimates for 3x simulated coverage when true error rates are given.

Cov.	AC	AG	AT	CG	CT	GT
1	1.99e-4	7.38e-4	9.21e-5	2.66e-4	6.13e-4	2.00e-4
2	1.12e-4	2.00e-4	8.03e-5	9.77e-5	2.48e-4	9.92e-5
3	9.34e-5	2.06e-4	1.00e-4	1.03e-4	1.97e-4	1.03e-4

Table 6: Genotype frequency estimates for 1-3x simulated average coverage. In contrast to the fixed coverage in the previous simulations, the simulated coverage follows a poisson distribution. Each simulation encompasses 10 million simulated sites, including sites that had no coverage.

Cov.	AC	AG	AT	CG	CT	GT	ref.bias
3	0.1071	0.2018	0.0989	0.094	0.1988	0.104	0.5511
4	0.0983	0.1951	0.1047	0.1017	0.199	0.098	0.5494
5	0.0983	0.1975	0.0975	0.0969	0.1965	0.1011	0.5461
6	0.096	0.203	0.0977	0.0977	0.1991	0.0996	0.5498
7	0.0993	0.1914	0.0976	0.1003	0.1969	0.0972	0.5464
8	0.0997	0.1981	0.0993	0.0992	0.201	0.0998	0.5475
9	0.1027	0.1996	0.0977	0.105	0.2007	0.097	0.5510
10	0.0958	0.2	0.0991	0.1047	0.2023	0.0966	0.5515
12	0.0976	0.2029	0.0985	0.0987	0.1966	0.0995	0.5508
15	0.0962	0.1955	0.0966	0.1	0.2036	0.1045	0.5501
17	0.1018	0.1918	0.0966	0.0953	0.202	0.0966	0.5503
20	0.1019	0.1963	0.0992	0.1039	0.1928	0.0958	0.5485
25	0.0964	0.2025	0.0946	0.0986	0.2072	0.1016	0.5488
30	0.0996	0.2049	0.1047	0.1009	0.1997	0.1044	0.5514

Table 7: Simulated genotype frequencies with reference bias (per 1000bp).

Cov.	AC	AG	AT	CG	CT	GT	ref.bias
3	1	1	1	1	1	1	0.95417
4	1	1	1	1	1	1	0.953826
5	1	1	1	1	1	1	0.956578
6	1	1	1	1	1	1	0.958906
7	1	1	1	1	1	1	0.958269
8	1	1	1	1	1	1	0.953793
9	1	1	1	1	1	1	0.950293
10	0.103956	0.251935	0.107054	0.115078	0.252771	0.104944	0.608715
12	0.0993383	0.22121	0.0997244	0.101436	0.21645	0.102138	0.5730837
15	0.0977169	0.202107	0.0976777	0.100955	0.210079	0.104663	0.558126
17	0.101805	0.197107	0.0978276	0.096013	0.203464	0.0969439	0.5546397
20	0.101403	0.198897	0.0989341	0.104611	0.195179	0.0956663	0.5505485
25	0.0970535	0.201382	0.0935319	0.0976879	0.20715	0.101026	0.549275
30	0.0996463	0.20537	0.104621	0.101775	0.202138	0.104083	0.5518523

Table 8: Estimated genotype frequencies (per 1000bp) and reference bias from simulations with reference bias (see Table 7). Frequencies of 1/1000bp correspond to the initial values for the optimization procedure and indicate that the algorithm did not converge.

Cov.	AC	AG	AT	CG	CT	GT	ref.bias
3	1	1	1	1	1	1	0.953438
4	1	1	1	1	1	1	0.953484
5	1	1	1	1	1	1	0.956395
6	1	1	1	1	1	1	0.958075
7	1	1	1	1	1	1	0.956719
8	1	1	1	1	1	1	0.95392
9	0.103322	0.237223	0.0982436	0.104155	0.234996	0.103418	0.5754379
10	0.105007	0.207003	0.0977101	0.103477	0.22399	0.103373	0.5405103
12	0.10596	0.208124	0.0997445	0.0944469	0.20766	0.100264	0.518081
15	0.100901	0.20544	0.100627	0.0985946	0.197782	0.102163	0.50840239
17	0.10114	0.202382	0.0990932	0.0991423	0.202261	0.0962275	0.50315541
20	0.0986462	0.194231	0.102811	0.0999103	0.200908	0.103067	0.5000655172
25	0.104676	0.19986	0.0975324	0.0960198	0.201889	0.0984695	0.50172859
30	0.0975958	0.204819	0.10192	0.0974037	0.201259	0.0976113	0.50130228

Table 9: Estimated genotype frequencies (per 1000bp) and reference bias from simulations without reference bias (see Table 2). Simulations included no reference bias ($r = 0.50$), but fluctuated between 0.498-0.502 due to the use of a pseudo random number generator.

Genotype	Previous estimates	Current estimates	Exp-Obs/Exp
AC	0.02637483448	0.0266535	-0.0106
AG	0.08703966695	0.0871984	-0.0018
AT	0.02642543445	0.0267161	-0.0110
CG	0.02333611154	0.0235279	-0.0082
CT	0.08398376852	0.0839987	-0.0002
GT	0.02822805388	0.028621	-0.0139

Table 10: Vindija 33.19: previous and new genotype frequency estimates for 30x chromosome 21. Previous estimates were based on an error rates derived from comparing Vindija 33.19 sequences to the Altai Neandertal genotypes, while the new procedure co-estimates the error. Genotype frequencies are given per 1000bp.

Cov.	AC	AG	AT	CG	CT	GT
1	0.156481	1	0.099432	0.181886	1	0.148702
2	0.0235957	0.0915316	0.00995462	0.0212318	0.0902833	0.0243273
3	0.0194142	0.0793266	0.015004	0.0183244	0.0831413	0.0229132
4	0.0230869	0.0873542	0.0164465	0.0204864	0.0896604	0.0222243
5	0.022984	0.0841431	0.017246	0.0208929	0.0846063	0.0221146
6	0.0225169	0.0834912	0.016566	0.0198478	0.0836662	0.022483
7	0.0222535	0.0854938	0.0175251	0.0195863	0.0812381	0.022945
8	0.0218176	0.087055	0.0177506	0.0197764	0.0823211	0.0221323
9	0.0228057	0.0861142	0.0181263	0.0209766	0.0837547	0.0230667
10	0.0220717	0.0843099	0.0190784	0.0205518	0.0859023	0.0233493
12.5	0.0238188	0.0871949	0.0201923	0.0209605	0.0845151	0.0239949
15	0.0237837	0.0878583	0.020731	0.0214662	0.0845611	0.0245654
17.5	0.0247929	0.0860958	0.0219419	0.0216504	0.0842108	0.0253737
20	0.0241059	0.0887325	0.0234373	0.0222888	0.0844751	0.0255594
25	0.0260217	0.0867229	0.0250622	0.0230925	0.0845706	0.0275897
30	0.0266535	0.0871984	0.0267161	0.0235279	0.0839987	0.028621

Table 11: Estimated genotype frequencies (per 1000bp) for subsampled Vindija 33.19 data and full data (30-fold coverage) for Chromosome 21.

Cov.	AC	AG	AT	CG	CT	GT	ref.bias.
1	1	1	1	1	1	1	0.488789
2	1	1	1	1	1	1	0.483124
3	1	1	1	1	1	1	0.482451
4	1	1	1	1	1	1	0.483107
5	1	1	1	1	1	1	0.483965
6	1	1	1	1	1	1	0.484572
7	1	1	1	1	1	1	0.484614
8	1	1	1	1	1	1	0.484388
9	1	1	1	1	1	1	0.48411
10	1	1	1	1	1	1	0.48357
12.5	0.0254813	0.102948	0.0211019	0.0233485	0.0974866	0.0260767	0.0780759
15	0.0250461	0.095778	0.0220548	0.0220069	0.0927085	0.0257213	0.0641697
17.5	0.0255528	0.0917879	0.0226941	0.0221606	0.0896427	0.0262666	0.055925
20	0.026011	0.0911584	0.0243382	0.0229291	0.0882428	0.0274094	0.0526592
25	0.0265753	0.0896112	0.0260777	0.0234638	0.0872355	0.0283603	0.0495509
30	0.0271757	0.0892411	0.0278416	0.0238781	0.086252	0.0291206	0.0471163

Table 12: Estimated genotype frequencies (per 1000bp) and reference bias for subsampled Vindija 33.19 data and full data (30-fold coverage) for Chromosome 21.

Genotypes	1x	2x	3x	4x	5x	6x	7x	8x	9x	10x	12.5x	15x	17.5x	20x	25x
0/0:0/1	5152	63	94	180	222	247	284	306	313	318	303	259	228	194	130
0/0:1/1	99102	84857	55902	34348	20669	12343	7623	4773	3022	1981	784	370	204	122	43
0/0:1/2	8	0	0	0	1	0	0	0	0	0	0	0	0	0	0
0/1:0/0	1711	2542	2632	2469	2230	1975	1748	1559	1362	1191	892	687	544	404	203
0/1:1/1	19	15	13	8	8	5	4	4	3	3	2	1	1	0	0
0/1:1/2	2	0	0	0	0	0	0	0	0	0	0	0	0	0	0
1/1:0/0	197	192	149	108	89	64	51	49	50	51	45	39	37	28	11
1/1:1/2	7	0	0	0	0	0	0	1	1	1	1	1	2	2	2
1/2:0/0	0	1	2	1	1	1	1	0	0	1	1	0	0	0	0
1/2:0/1	0	0	0	1	1	1	1	2	2	2	2	2	1	0	2
1/2:1/1	9	12	15	19	18	19	20	23	24	25	26	23	19	18	6
concordant 0/0	14054746	19237587	21245357	22061259	22419936	22585939	22664220	22703546	22723853	22735585	22747418	22751474	22753357	22754464	22755575
concordant 0/1	1845	2468	2936	3339	3711	4039	4308	4535	4754	4940	5261	5471	5616	5760	5964
concordant 1/1	21578	29995	33441	35026	35754	36169	36402	36508	36612	36681	36801	36897	36981	37040	37159
concordant 1/2	0	0	0	1	3	4	5	6	6	6	5	9	14	16	26
discordant 0/1	1	0	0	2	2	1	1	1	1	1	2	4	3	2	0
discordant 1/1	68	53	57	37	25	17	15	16	14	16	22	23	17	11	6

Table 13: Comparison of called genotypes in Vindija 33.19 subsamples to 30x calls. Genotypes column give the combination of genotypes in order 30x:subsample. Discordant genotypes list the events where the state matched, but the called alleles differed.

Genotypes	1x	2x	3x	4x	5x	6x	7x	8x	9x	10x	12.5x	15x	17.5x	20x	25x
0/0:0/1	9	1	1	0	0	1	1	2	2	1	0	1	1	1	0
0/0:1/1	1515	1878	1299	806	463	290	169	114	73	40	13	3	0	0	0
0/1:0/0	266	774	735	628	528	411	332	270	246	204	134	87	52	29	5
0/1:1/1	1	0	0	0	0	0	0	0	0	0	0	0	0	0	0
1/1:0/0	8	7	4	5	3	0	0	0	0	0	0	0	0	0	0
1/2:0/1	0	0	0	0	0	0	0	1	1	0	0	0	0	0	0
1/2:1/1	0	3	6	5	4	3	2	3	3	2	1	1	1	1	0
concordant 0/0	4298057	13965648	17863618	20021659	21188632	21822227	22167988	22364540	22483197	22557762	22653561	22695379	22717659	22730345	22742667
concordant 0/1	217	694	767	916	1132	1447	1847	2225	2589	2946	3702	4254	4641	4941	5321
concordant 1/1	5573	20989	27162	30751	32771	33982	34655	35098	35375	35587	35903	36096	36234	36313	36450
concordant 1/2	0	0	0	1	1	2	2	2	3	4	4	5	9	10	10
discordant 1/1	1	2	4	2	1	0	0	0	0	0	0	0	0	0	0

Table 14: Comparison of called genotypes of at least GQ30 in Vindija 33.19 subsamples to 30x calls. Labels as in Table 13.

Genotypes	1x	2x	3x	4x	5x	6x	7x	8x	9x	10x	12.5x	15x	17.5x	20x	25x
0/0:0/1	0	0	0	0	0	0	0	0	0	0	0	1	0	0	0
0/1:0/0	0	19	42	50	60	47	56	49	44	34	26	18	6	2	0
1/2:1/1	0	0	0	0	0	1	1	1	1	1	0	0	0	0	0
concordant 0/0	748	1241358	3509091	6215502	9257342	12043092	14401637	16302760	17780674	18908590	20692904	21590412	22064492	22322058	22565822
concordant 0/1	4	31	89	222	398	617	949	1272	1615	2030	2900	3586	4107	4490	5011
concordant 1/1	4	1394	4170	7831	12069	16264	19988	23158	25644	27635	30965	32820	33917	34557	35347
concordant 1/2	0	0	0	0	0	1	1	2	2	2	4	5	5	5	6

Table 15: Comparison of called genotypes of at least GQ50 in Vindija 33.19 subsamples to 30x calls. Labels as in Table 13.

Genotype	Vindija 33.15 without ref.bias	Vindija33.15 with ref.bias
AC	0.0266134	0.0287228
AG	0.0963167	0.109077
AT	0.0244506	0.0271335
CG	0.0233174	0.0246703
CT	0.0962895	0.110025
GT	0.0257977	0.0272471

Table 16: Vindija 33.15: genotype frequency estimates with and without reference bias. The estimated reference bias for the third column was 10.14% ($r = 0.6014$). Genotype frequencies are given per 1000bp.

GT Vi.33.15	GT Vi.33.19	¬RB vs. ¬RB	RB vs. ¬RB	¬RB vs. RB	RB vs. RB
0/0	0/0	17461981	17461610	17461954	17461583
0/0	0/1	112	102	139	129
0/0	1/1	1	1	1	1
0/1	0/0	352	722	347	717
0/1	0/1	3785	3793	3790	3798
0/1	1/1	79	39	79	39
1/1	0/0	1	2	1	2
1/1	0/1	12	14	12	14
1/1	1/1	26117	26157	26117	26157
1/2	1/1	1	1	1	1
1/2	1/2	5	5	5	5

Table 17: Comparison of Vindija 33.19 and 33.15 chr21 genotypes with and without reference bias. The samples Vindija 33.19 and 33.15 have been found to originate from the same individual. The first two columns shows the observed configuration of genotypes. The remaining columns show the counts of genotypes of each configuration observed when calling Vindija 33.15 and Vindija 33.19 with (RB) or without (¬RB) taking reference bias into account. Parameter estimates for genotype frequencies with and without reference bias are listed in Tables 12 and 11, respectively, for Vindija 33.19 and in Table 16 for Vindija 33.15.

Vi33.19 coverage	AC	AG	AT	CG	CT	GT
0.9x	0.0195129	0.109353	0.0205452	0.0187133	0.11283	0.022431
1.0x	0.0193746	0.100528	0.0202986	0.0174671	0.101193	0.0219828
1.2x	0.0191059	0.092621	0.0208953	0.0169481	0.0982858	0.0200446
1.5x	0.0188508	0.0847961	0.0201072	0.016174	0.0860951	0.0185336
2.0x	0.0189877	0.0808416	0.0205732	0.0161658	0.0862022	0.0179353
30x*	0.0197930	0.065936	0.0205161	0.0195035	0.0646958	0.0203278

Table 18: Estimated genotype frequencies (per 1000bp) for subsampled Vindija 33.19 data and full data (30-fold coverage) for autosomal sites with at least 4-fold coverage. * 30x coverage estimate is the average, weighted by chromosome size, of the previously published genotype frequencies.

Vi33.19 coverage	AC	AG	AT	CG	CT	GT
Goyet	0.0167772	0.058848	0.0183608	0.0169625	0.0592227	0.0181386
LesCottés	0.0195414	0.0562096	0.0269036	0.014648	0.0600958	0.0209159
Mez2	0.017562	0.0569594	0.0176347	0.0175739	0.0576068	0.0180015
Vindija87	0.0201796	0.0758009	0.0240558	0.0203436	0.0809328	0.022701
Spy	0.031233	0.0893976	0.0394828	0.0264985	0.0949992	0.031182
Loschbour 1x	0.0510422	0.19892	0.0425446	0.0373921	0.195768	0.0535498
Loschbour 2x	0.0510101	0.201208	0.0409543	0.0388374	0.202462	0.052122
Motala12	0.0549699	0.260431	0.0425594	0.0612579	0.259056	0.0556023
Loschbour 22x*	0.05067	0.20966	0.04319	0.05325	0.20831	0.05103

Table 19: Estimated genotype frequencies (per 1000bp) for low-coverage archaic and modern human data on autosomes for sites with at least 4-fold coverage. * Genome-wide average, weighted by chromosome sizes, of previous snpAD estimates.

Parameter	No mapability	map35_100
depth	1.83309693	0.859994221
fracMissing	0.44624482	0.728850233
fracTwoOrMore	0.55375518	0.271149767
pi(A)	0.233486339	0.217336017
pi(C)	0.245584846	0.262575431
pi(G)	0.262368764	0.283677311
pi(T)	0.258560051	0.236411241
theta_MLE	0.00218729023	0.00123814321
theta_C95_l	0.00177227373	0.000745217841
theta_C95_u	0.00260230673	0.00173106857
LL	-241726.674	-117295.226

Table 20: ATLAS' genome-wide estimates of θ for Motala12 with and without mapability track.

3 Comparison to GATK and samtools

3.1 Altai Neandertal Chromosome 21

Previous analyses used GATK to call genotypes for the high-coverage Denisovan and Altai Neandertal genomes (Meyer *et al.*, 2012; Prüfer *et al.*, 2014). Both genomes were treated with an enzyme to remove most of the ancient DNA damage (Briggs *et al.*, 2010), leaving only the first and last two bases of sequences to carry elevated C to T exchanges.

To test whether an earlier version of snpAD improves the genotypes for these genomes, the calls of GATK were previously compared to those from snpAD for the Altai Neandertal chromosome 21 (Prüfer *et al.*, 2017). This chromosome contains an ≈19Mb long region that appears nearly devoid of heterozygous sites. The presence of such regions in the genome of the Altai Neandertal indicates that the individuals parents were closely related (at the level of half-siblings), causing long regions of homozygosity in the offspring (Prüfer *et al.*, 2014). The comparison of snpAD and GATK showed that snpAD calls a significantly smaller fraction of heterozygous sites in the inbred region than GATK. Note that the inbred regions were discovered based on the GATK calls and are therefore expected to be biased in favor of low heterozygosity in these calls.

Repeating this analysis, the Altai chromosome 21 was re-genotyped with the latest snpAD version. As before, single and double stranded libraries were regarded separately. The software was otherwise run with default parameters. Both GATK and snpAD calls were filtered according to the minimal recommended filters. Table 21 shows that snpAD continues to call a significantly lower fraction of heterozygous sites in the inbred region, where few to no heterozygous sites are expected (Fisher's exact test $p < 2 \times 10^{-9}$).

MapDamage can process bam files to lower the quality of bases that may be affected by ancient DNA damage. To test whether this approach yields an improvement, the quality scores in the Altai chromosome 21 bam file were rescaled with mapDamage (version: 2.0.2-6-gdb9ad80) using the option `--single-stranded` followed by genotyping with GATK as described before (Prüfer *et al.*, 2014). The number of heterozygous sites called by GATK are lower after rescaling than without rescaling. Their distribution in inbred and non-inbred regions does not differ significantly between rescaled GATK calls and GATK calls based on sequences where T's at the first or last two positions were masked ($p > 0.6$). As for the non-rescaled GATK calls, snpAD calls show a significantly smaller fraction of heterozygous sites in inbred regions compared to the rescaled GATK calls ($p < 4 \times 10^{-8}$; Table 21).

To test whether GATK calls could be improved by applying a genotype quality cutoff (QUAL field), I tested increasing cutoffs (steps of 10) until the number of rescaled GATK heterozygous sites for the inbred region were close to the number of snpAD calls. At QUAL $\geq$ 590, GATK+mapDamage yielded 92 heterozygote calls (QUAL$\geq$600 yielded 90). However, this cutoff also led to a substantial decrease in called heterozygotes outside of the inbred region (GATK called 35% less heterozygotes compared to snpAD; see Table 21; Fisher's exact test of ratios $p = 0.004$). The difference between snpAD and GATK in called heterozygotes between inbred and non-inbred region can thus not be eliminated by applying quality cutoffs on GATK genotypes.

Genotype calls were also produced by running samtools (version: 1.3.1-21-g874baf3) followed by bcftools (version: 1.4) with the options "-c" (consensus caller) or "-m" (multiallelic caller). The samtools genotyping was run with and without quality score rescaling using mapDamage. All VCFs were filtered using the minimal recommended filters for the Altai Neandertal. No significant difference in the ratio of heterozyzgous calls within and outside of the inbred region was detected in comparison to snpAD, indicating a similar quality of calls.

Genotyper	inbred	non-inbred	p-value to snpAD
snpAD	91	2291	-
GATK	501	2689	$< 2 \times 10^{-16}$
GATK*	206	2431	2×10^{-9}
GATK+mapDamage	191	2387	4×10^{-8}
GATK+mapDamage (QUAL≥590)	92	1497	4×10^{-3}
samtools (-c)	96	2293	0.78
samtools (-m)	84	2280	0.64
samtools+mapDamage (-c)	95	2298	0.82
samtools+mapDamage (-m)	88	2281	0.88

Table 21: GATK and samtools vs. snpAD heterozygous calls within and outside of an autozygous region on Altai chromosome 21. The region spans bases chr21:17081807-35881807 in hg19 coordinates. Brackets after samtools give the option used for calling with bcftools. Column "p-value" shows the result of a Fisher's exact test of the inbred/non-inbred counts against the counts for snpAD. * These calls for GATK were based on a modified input file in which T's at the first and last two positions were masked (see also (Prüfer *et al.*, 2017)).

3.2 Vindja 33.19 Neandertal Chromosome 21

Due to the enzyme treatment, few erroneous C to T exchanges remain in the sequences of the high-coverage Altai Neandertal. In contrast, only a quarter of the high-coverage Vindija 33.19 Neandertal data come from enzyme treated libraries, resulting in common C to T exchanges in the majority of sequences. To test how the snpAD calls compare to those produced by other genotyper-software for this more challenging dataset, I ran samtools and GATK with and without mapDamage quality score rescaling on the chromosome 21 data of Vindija 33.19. MapDamage rescaling was run separately for the data of treated and untreated libraries using the option `--single-stranded`. All VCF files were restricted to sites that pass the recommended minimum filters for Vindija 33.19 (Prüfer *et al.*, 2017).

Table 22 shows the number of called heterozygous sites for all runs together with the transition/transversion (ts/tv) ratio of these sites. SnpAD yielded with 2.06 the lowest ts/tv ratio among all runs. Note that this value falls within the range of ts/tv ratios observed for GATK calls of 25 modern human genomes of diverse ancestry (1.95-2.17; A and B-panel from Meyer *et al.* (2012) and Prüfer *et al.* (2014)). For the remaining genotypers, the calls with mapDamage rescaling are consistently smaller in their ts/tv ratios than those without, indicating that mapDamage is reducing the influence of C to T exchanges. However, even after correction the ts/tv values fall outside of the range observed in present-day human genomes, suggesting that the calls still contain a large number of errors due to ancient DNA damage.

Genotyper	AC	AG	AT	CG	CT	GT	ts/tv
snpAD	441	1638	335	390	1645	424	2.06
GATK	472	114789	370	406	115047	449	135.44
GATK+mapDamage	472	8496	370	406	8703	449	10.13
samtools (-c)	415	6188	287	376	6281	395	8.47
samtools+mapDamage (-c)	415	3927	288	376	3999	395	5.38
samtools (-m)	414	4363	284	375	4380	390	5.98
samtools+mapDamage (-m)	414	3022	285	374	3018	391	4.13

Table 22: GATK and samtools vs. snpAD heterozygous calls on Vindija 33.19 chromosome 21. Shown are the number of heterozygous calls for each genotype. Column ts/tv gives the transition/transversion ratio. The ts/tv ratio of snpAD is significantly lower than those of all other genotypers (Fisher's exact test on the ts and tv counts: $p < 2.2 \times 10^{-16}$ for all pairwise tests)

4 Comparison to ATLAS

ATLAS 1.0 was downloaded on 2017-11-23 from the authors github page (rev. 9b2390c). Conserved regions were downloaded according to the authors instructions and modified to fit the coordinates in bam files:

```
cat original_hg19_UCNE_coord.bed |
        sed -e 's/^chr//g' > hg19_UCNE_coord.bed
```

ATLAS was then run with the *recal* option using the following steps:

```
atlas task=estimatePMD bam=motala12.bam \
        fasta=hg19_evan/whole_genome.fa \
        length=25

atlas task=recal bam=motala12.bam \
        pmdFile=motala12_PMD_input_Empiric.txt \
        regions=hg19_UCNE_coord.bed verbose

atlas task=recalBAM bam=motala12.bam \
        recal=motala12_recalibrationEM.txt \
        pmdFile=motala12_PMD_input_Empiric.txt \
        fasta=hg19_evan/whole_genome.fa \
        withPMD maxOutQuality=42 verbose
```

The resulting recalibrated quality scores appeared to shift all quality scores to values less than 10:

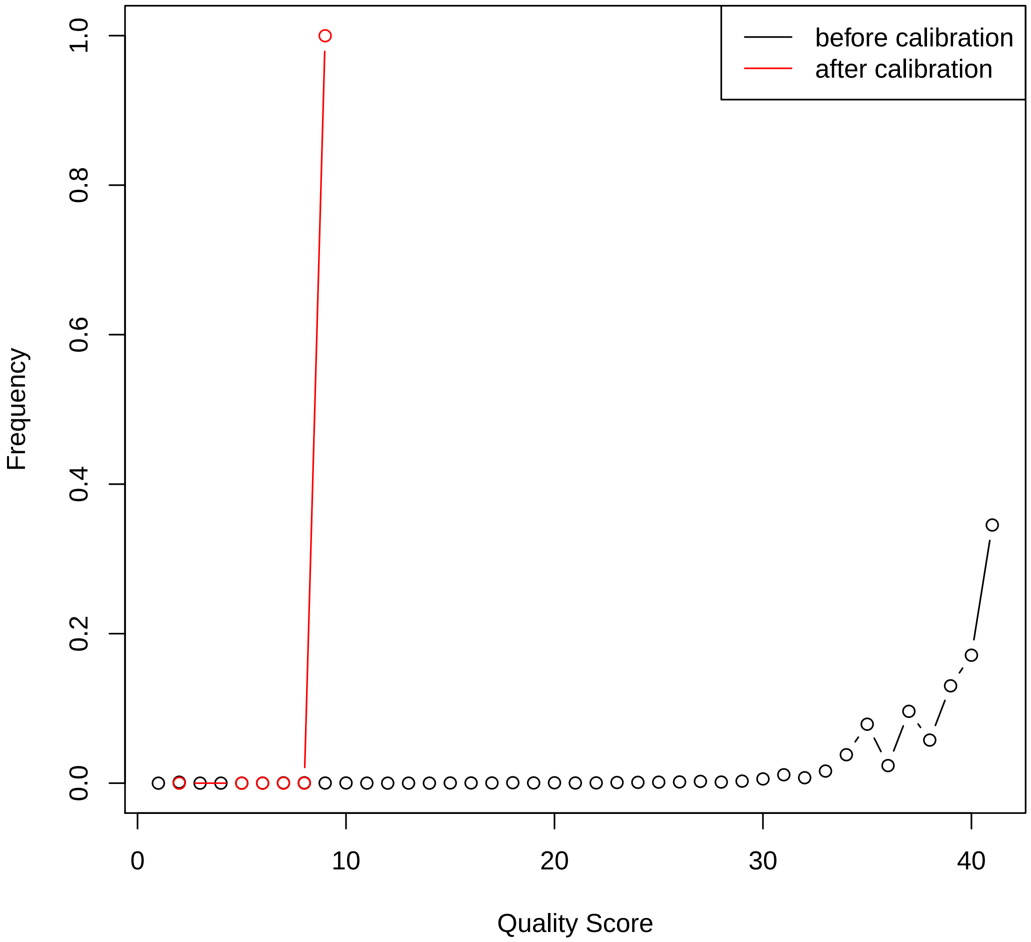

Running ATLAS with the *minDepth=2* option did not change the result.

A new version of ATLAS 1.0 was downloaded on 2018-03-15 (commit 49f1fea). PMD estimation was run with the command:

```
atlas task=estimatePMD \
        bam=motala12.bam \
        fasta=hg19_evan/whole_genome.fa \
        length=25
```

The command failed with the message ”Error: Length mismatch!”.

Using the previous estimates of the older ATLAS version for the *estimatePMD* step, the following commands were run:

```
atlas task=recal bam=motala12.bam \
        pmdFile=motala12_PMD_input_Empiric.txt \
        regions=hg19_UCNE_coord.bed verbose

atlas task=recalBAM bam=motala12.bam \
        recal=motala12_recalibrationEM.txt \
        pmdFile=motala12_PMD_input_Empiric.txt \
        fasta=hg19_evan/whole_genome.fa withPMD \
        maxOutQuality=42 verbose
```

The execution of *recalBAM* failed with the same message as before, but left an indexable recalibrated bam file with a more reasonable quality score distribution:

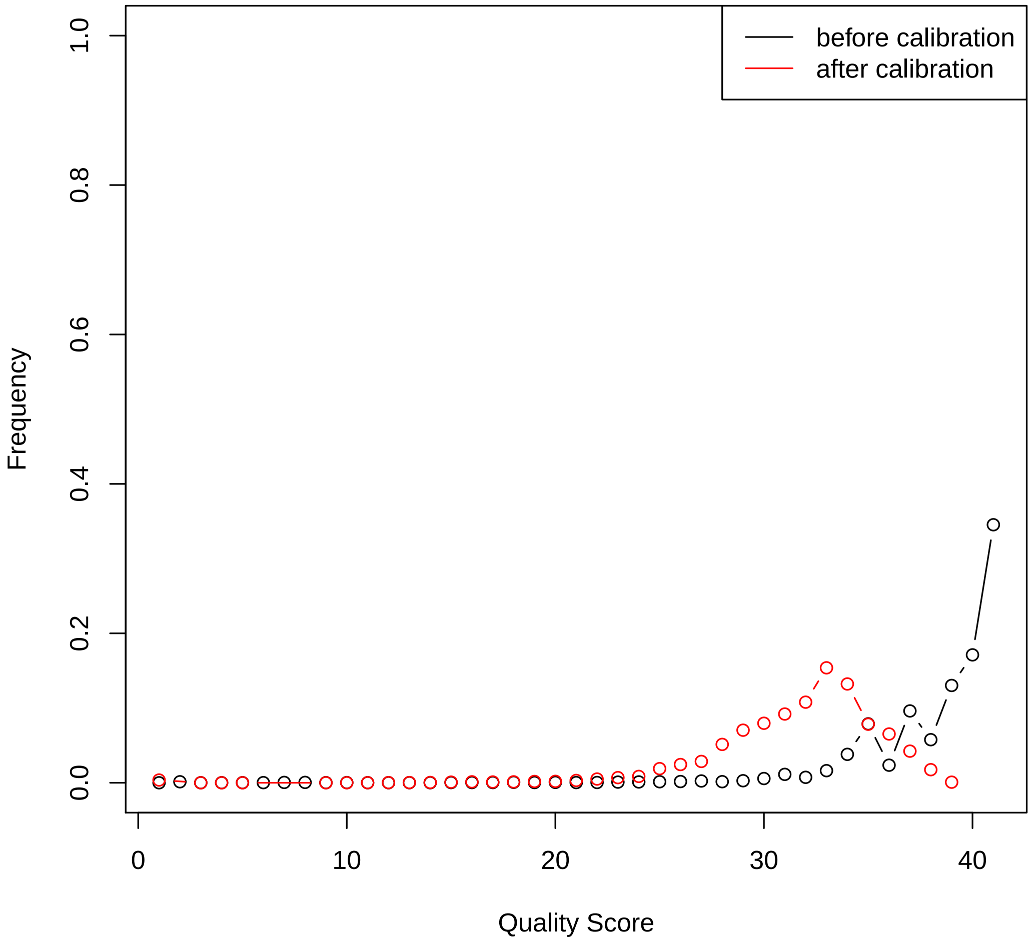

Genome-wide theta on the autosomes were estimated for all regions and for regions passing a 35mer mapability filter (map35_100) that was used in the analysis of the Altai Neandertal and Vindija Neandertal, and for all snpAD estimates in this paper:

```
atlas task=estimateTheta bam=motala12.bam \
        pmdFile=motala12_PMD_input_Empiric.txt \
        recal=motala12_recalibrationEM.txt \
        thetaGenomeWide limitChr=22 \
        minDepth=2 verbose

atlas task=estimateTheta bam=motala12.bam \
        pmdFile=motala12_PMD_input_Empiric.txt \
        recal=motala12_recalibrationEM.txt \
        thetaGenomeWide limitChr=22 \
        regions=hs37m_filt35_99.bed.gz \
        minDepth=2 verbose
```

The resulting estimates are shown in Table 20.

References

Briggs, A. W., Stenzel, U., Meyer, M., Krause, J., Kircher, M., and Pääbo, S. (2010). Removal of deaminated cytosines and detection of in vivo methylation in ancient DNA. *Nucleic Acids Research*, **38**(6), e87.

Hajdinjak, M., Fu, Q., Hübner, A., Petr, M., Mafessoni, F., Grote, S., Skoglund, P., Narasimham, V., Rougier, H., Crevecoeur, I., Semal, P., Soressi, M., Talamo, S., Hublin, J.-J., Gušić, I., Kućan, Ž., Rudan, P., Golovanova, L. V., Doronichev, V. B., Posth, C., Krause, J., Korlević, P., Nagel, S., Nickel, B., Slatkin, M., Patterson, N., Reich, D., Prüfer, K., Meyer, M., Pääbo, S., and Kelso, J. (2018). Reconstructing the genetic history of late Neanderthals. *Nature*, page in press.

Lazaridis, I., Patterson, N., Mittnik, A., Renaud, G., Mallick, S., Kirsanow, K., Sudmant, P. H., Schraiber, J. G., Castellano, S., Lipson, M., Berger, B., Economou, C., Bollongino, R., Fu, Q., Bos, K. I., Nordenfelt, S., Li, H., de Filippo, C., Prüfer, K., Sawyer, S., Posth, C., Haak, W., Hallgren, F., Fornander, E., Rohland, N., Delsate, D., Francken, M., Guinet, J.-M., Wahl, J., Ayodo, G., Babiker, H. A., Bailliet, G., Balanovska, E., Balanovsky, O., Barrantes, R., Bedoya, G., Ben-Ami, H., Bene, J., Berrada, F., Bravi, C. M., Brisighelli, F., Busby, G. B. J., Cali, F., Churnosov, M., Cole, D. E. C., Corach, D., Damba, L., van Driem, G., Dryomov, S., Dugoujon, J.-M., Fedorova, S. A., Gallego Romero, I., Gubina, M., Hammer, M., Henn, B. M., Hervig, T., Hodoglugil, U., Jha, A. R., Karachanak-Yankova, S., Khusainova, R., Khusnutdinova, E., Kittles, R., Kivisild, T., Klitz, W., Kučinskas, V., Kushniarevich, A., Laredj, L., Litvinov, S., Loukidis, T., Mahley, R. W., Melegh, B., Metspalu, E., Molina, J., Mountain, J., Näkkäläjärvi, K., Nesheva, D., Nyambo, T., Osipova, L., Parik, J., Platonov, F., Posukh, O., Romano, V., Rothhammer, F., Rudan, I., Ruizbakiev, R., Sahakyan, H., Sajantila, A., Salas, A., Starikovskaya, E. B., Tarekegn, A., Toncheva, D., Turdikulova, S., Uktveryte, I., Utevska, O., Vasquez, R., Villena, M., Voevoda, M., Winkler, C. A., Yepiskoposyan, L., Zalloua, P., Zemunik, T., Cooper, A., Capelli, C., Thomas, M. G., Ruiz-Linares, A., Tishkoff, S. A., Singh, L., Thangaraj, K., Villems, R., Comas, D., Sukernik, R., Metspalu, M., Meyer, M., Eichler, E. E., Burger, J., Slatkin, M., Pääbo, S., Kelso, J., Reich, D., and Krause, J. (2014). Ancient human genomes suggest three ancestral populations for present-day Europeans. *Nature*, **513**(7518), 409–413.

Meyer, M., Kircher, M., Gansauge, M.-T., Li, H., Racimo, F., Mallick, S., Schraiber, J. G., Jay, F., Prüfer, K., Filippo, C. d., Sudmant, P. H., Alkan, C., Fu, Q., Do, R., Rohland, N., Tandon, A., Siebauer, M., Green, R. E., Bryc, K., Briggs, A. W., Stenzel, U., Dabney, J., Shendure, J., Kitzman, J., Hammer, M. F., Shunkov, M. V., Derevianko, A. P., Patterson, N., Andrés, A. M., Eichler, E. E., Slatkin, M., Reich, D., Kelso, J., and Pääbo, S. (2012). A High-Coverage Genome Sequence from an Archaic Denisovan Individual. *Science*, **338**(6104), 222–226.

Prüfer, K., Racimo, F., Patterson, N., Jay, F., Sankararaman, S., Sawyer, S., Heinze, A., Renaud, G., Sudmant, P. H., de Filippo, C., Li, H., Mallick, S., Dannemann, M., Fu, Q., Kircher, M., Kuhlwilm, M., Lachmann, M., Meyer, M., Ongyerth, M., Siebauer, M., Theunert, C., Tandon, A., Moorjani, P., Pickrell, J., Mullikin, J. C., Vohr, S. H., Green, R. E., Hellmann, I., Johnson, P. L. F., Blanche, H., Cann, H., Kitzman, J. O., Shendure, J., Eichler, E. E., Lein, E. S., Bakken, T. E., Golovanova, L. V., Doronichev, V. B., Shunkov, M. V., Derevianko, A. P., Viola, B., Slatkin, M., Reich, D., Kelso, J., and Pääbo, S. (2014). The complete genome sequence of a Neandertal from the Altai Mountains. *Nature*, **505**(7481), 43–49.

Prüfer, K., de Filippo, C., Grote, S., Mafessoni, F., Korlević, P., Hajdinjak, M., Vernot, B., Skov, L., Hsieh, P., Peyrégne, S., Reher, D., Hopfe, C., Nagel, S., Maricic, T., Fu, Q., Theunert, C., Rogers, R., Skoglund, P., Chintalapati, M., Dannemann, M., Nelson, B. J., Key, F. M., Rudan, P., Kućan, Ž., Gušić, I., Golovanova, L. V., Doronichev, V. B., Patterson, N., Reich, D., Eichler, E. E., Slatkin, M., Schierup, M. H., Andrés, A. M., Kelso, J., Meyer, M., and Pääbo, S. (2017). A high-coverage Neandertal genome from Vindija Cave in Croatia. *Science (New York, N.Y.)*, **358**(6363), 655–658.